Table 1. Patient characteristics, clinical manifestations, and outcomes

Patient	Age (Months)	Sex	Prodromal Infection*	Initial Neurologic Signs	LOC on Next Day
1	45	F	URI (9)	LOC alone	Mild
2	156	M	NSFI (2)	Brief SZ	Subtle
3	28	M	Enterocolitis‡ (6)	Prolonged SZ	Mild
4	32	M	NSFI (0)	Delirious behavior	Subtle
5	33	F	URI (1)	Brief SZ	Subtle
6	37	M	NSFI (0)	Prolonged SZ	Mild
7	44	F	Influenza A (0)	Prolonged SZ	Mild
8	60	M	Influenza A (0)	Brief SZ	Mild
9	44	F	Influenza A (0)	Brief SZ	Subtle

* Numbers in parentheses indicate interval between prodromal illness and onset of encephalopathy.
† Numbers in parentheses indicate days after onset.
‡ Verotoxin-producing *Escherichia coli* were isolated from stool.
§ Oral tendency was also observed 20 days after onset.

Abbreviations:
F = Female
LOC = Loss of consciousness
M = Male
NSFI = Nonspecific febrile illness
SZ = Seizure
URI = Upper respiratory infection

Patients and Methods

We reviewed the hospital records of patients with acute encephalopathy who were admitted to the Department of Pediatrics in Nagoya University Hospital (Nagoya, Aichi, Japan) and its affiliated 12 hospitals between January 1998 and March 2005. We identified 97 patients with acute encephalopathy, as characterized by decreased consciousness with or without other neurologic signs lasting for >24 hours in children with infectious symptoms. We carefully excluded patients with sustained decreased consciousness after a febrile seizure, or those with delirious behavior without obvious reduced consciousness.

We assessed the detailed clinical course of each patient on the basis of medical records. We paid attention to initial neurologic signs, and the severity and time course of decreased consciousness. Nine (9%) of 97 patients fulfilled the following conditions: (1) mildly decreased consciousness on the day after onset, (2) deterioration of consciousness a few days after onset, and (3) no other cause of encephalopathy such as electrolyte derangement, metabolic abnormalities, or worsening of systemic diseases. These nine patients were the subjects of this study.

In this study, the initial neurologic signs were divided into the following four items: prolonged seizure, brief seizure, delirious behavior, and decreased consciousness alone. A prolonged seizure was defined as lasting for >20 minutes. A brief seizure was defined as those <20 minutes, irrespective of the number of seizures. Delirious behavior was defined as disoriented and incoherent action or speech lasting for >30 minutes. It may include visual hallucinations, irritability, fearful responses, and sensory misperception. Coma was defined as a condition in which a patient could not be aroused by maximal painful stimulation. This is consistent with a score of 3-5 in the Glasgow Coma Scale-Modified for Children or a score of 100-300 on the Japan Coma Scale. Semicoma was defined as a condition in which a patient could be aroused by painful stimulation. The loss of consciousness on the day after onset was milder than in most of these patients. Thus, we defined mild loss of consciousness as the condition in which a patient tended to be asleep but could be aroused without painful stimulation, and subtle loss of consciousness as the condition in which a patient remained awake but lacked spontaneity, or seemed absent-minded or slightly disoriented.

Laboratory data were also assessed through medical records. The following values were investigated: aspartate aminotransferase, alanine aminotransferase, lactate dehydrogenase, creatinine kinase, glucose, ammonia, and cell counts and protein in cerebrospinal fluid. All findings of cranial computed tomography and magnetic resonance imaging were evaluated retrospectively by 17 pediatric neurologists who were unaware of patients' detailed clinical courses. Single-photon emission tomography and electroencephalograms were interpreted by pediatric neurologists in each hospital.

All patients were followed by pediatric neurologists for at least 1 year. The severity of cognitive impairment was defined as mild when intelligence or developmental quotient was between 50-70, moderate when it was between 30-50, and severe when it was <30. The severity of motor impairment was defined as mild when a patient could walk with or without support, moderate when a patient could seat oneself without support, and severe when a patient could not seat oneself.

Results

Patient Characteristics

Patient characteristics are summarized in Table 1. Their median age was 44 months (range, 28-156 months). No patient was <2 years of age. No patient had a family history of febrile seizures, epilepsy, or other neurologic disorders. One patient (patient 4) manifested mild cognitive impairment and focal epilepsy of unknown origin. Three (patients 7, 8, and 9) had a past history of febrile seizures. The remaining 5 patients had no history of neurologic disorders.

The pathogen of prodromal infection was identified in 4 patients. Influenza A infection was virologically proven in 3 patients. Verotoxin-producing *Escherichia coli* were isolated in a stool sample from patient 3. In this patient, there were no clinical or laboratory findings suggesting an association with hemolytic-uremic syndrome. Prodromal illness involved upper respiratory infection in 2 patients, and nonspecific febrile illness without respiratory, urinary,

Table 1. Continued

Most Severe LOC†	Sz During Subacute Phase†	Behavioral Abnormalities†	Cognitive Impairment	Motor Impairment
Coma (3)	None	Stereotypic movement (3)	None	None
Coma (4)	Brief SZ (6)	None	Moderate	Mild
Semicoma (4)	None	Stereotypic movement (4)	Severe	None
Semicoma (7)	Clustered brief SZs (5)	None	Severe	Moderate
Coma (3)	Clustered brief SZs (4)	Oral automatic movement (6)‡	Moderate	Mild
Coma (3)	Prolonged SZ (7)	Oral tendency (18)	Severe	Mild
Coma (3)	None	Stereotypic movement (2)	Moderate	Mild
Coma (4)	None	Delirious behavior (3)	Mild	Mild
Coma (4)	Brief SZ (5)	None	None	Mild

or gastrointestinal signs in 3 patients. The interval between prodromal illness and onset of encephalopathy was <2 days in 7 patients. Theophylline had not been used in any of these patients before the onset of encephalopathy, whereas acetaminophen had been administered in 2 patients (patients 2 and 7).

Neurologic Signs and Clinical Courses

Neurologic signs and clinical courses are also listed in Table 1. The initial neurologic sign was a brief seizure in 4 patients, a prolonged seizure in 3, delirious behavior in 1, and loss of consciousness alone in 1. The severity of loss of consciousness on the next day of onset was subtle in 4 patients and mild in 5. However, worsening of consciousness was observed 3-7 days after onset. The most severe loss of consciousness was coma in 7 patients, and semicoma in 2.

During the subacute phase, seizures or behavioral abnormalities were present in all patients. Seizures were observed in 5 patients. A prolonged seizure was observed in 1 patient, clustered brief seizures in 2, and a single brief seizure in 2. Behavioral abnormalities were recognized in 6 patients. Stereotypic movements, such as purposeless hand movements, were recognized in 3 patients, oral tendency in 1, smacking-like oral automatic movements followed by an oral tendency in 1, and delirious behavior such as meaningless speech in 1.

Laboratory Data

In all but one patient, laboratory tests on admission revealed normal levels of aspartate aminotransferase, alanine aminotransferase, and creatinine kinase. One patient (patient 9) had mildly elevated levels of aspartate aminotransferase and alanine aminotransferase. Lactate dehydrogenase was mildly to moderately elevated in most patients on admission. These values reached peak levels on days 3-10 from the onset of encephalopathy. Marked elevations of aspartate aminotransferase (>200 IU/L) and alanine aminotransferase (>200 IU/L) were observed in 3 patients (patients 7-9), elevations of lactate dehydrogenase (>1000 IU/L) were observed in 3 (patients 5, 7, and 8), and elevations of creatinine kinase (>1000 IU/L) were observed in 2 (patients 2 and 6). Hyperammonemia, hypoglycemia, and metabolic or respiratory acidosis were not recognized in any patients. Cerebrospinal fluid analyses revealed mild pleocytosis with mildly increased protein levels in 3 patients (patients 1, 2, and 9).

Neuroradiologic Findings

Neuroradiologic findings are listed in Table 2. During the acute phase, computed tomography was performed in 6 patients, magnetic resonance imaging in 1, and both computed tomography and magnetic resonance imaging in 1. No abnormal findings were observed in these 8 patients.

During the subacute phase, when the worsening of consciousness had occurred, computed tomography was performed in 2 patients, magnetic resonance imaging in 3, and both computed tomography and magnetic resonance imaging in 3. No neuroradiologic examination was performed in 1 patient during this phase. Computed tomography demonstrated mild blurring of gray-white matter differentiation in the bilateral frontal areas of 2 patients (Fig 1). Magnetic resonance imaging revealed mild high

Table 2. Neuroradiologic findings

Patient	CT			MRI			SPECT
	Acute Phase	Subacute Phase	Late Phase	Acute Phase	Subacute Phase	Late Phase	
1	Normal (0)	Not performed	Not performed	Normal (1)	Normal (8)	Mild CA (40)	Not performed
2	Not done	Normal (7)	Normal (17)	Not performed	Normal (8)	Mild CA (33)	Hypoperfusion in bilateral F areas (11)
3	Normal (0)	Blurring of GWD in bilateral F areas (5)	Not performed	Not performed	HIA in bilateral F areas on T2WI/ FLAIR (14)	Mild CA (39)	Hypoperfusion in bilateral F-T areas (13)
4	Not done	Not performed	Not performed	Not performed	Normal (12)	Mild CA (34)	Diffuse hypoperfusion (20)
5	Normal (0)	Normal (4)	Not performed	Not performed	HIA in bilateral F areas on T2WI/ FLAIR (9)	Mild CA (23)	Hypoperfusion in bilateral F areas (22)
6	Normal (0)	Not performed	Not performed	Not performed	HIA in left T-P-O areas on DWI (9)	Mild CA (31)	Hypoperfusion in left T-P-O areas (16)
7	Normal (0)	Blurring of GWD in bilateral F areas (3)	Not performed	Not performed	Not performed	Mild CA (35)	Not performed
8	Normal (0)	Not performed	Mild CA (15)	Not performed	Not performed	Mild CA (21)	Not performed
9	Normal (0)	Normal (10)	Not performed	Normal (3)	Not performed	Normal (20)	Not performed

Numbers in parentheses indicate days after onset.

Abbreviations:
CA = Cortical atrophy
DWI = Diffusion-weighted images
F = Frontal
FLAIR = Fluid-attenuated inversion-recovery images
GWD = Gray-white matter differentiation
HIA = High-intensity area
O = Occipital
P = Parietal
T = Temporal
T2WI = T_2-weighted images

intensities in the bilateral frontal areas on T_2-weighted and fluid-attenuated inversion-recovery images in 2 patients (Fig 1), and marked high intensities in the left temporo-parieto-occipital area on diffusion-weighted images in 1 patient (Fig 2). No abnormalities were seen in 4 patients.

During the late phase, magnetic resonance imaging was performed in all 9 patients, and computed tomography was performed in 2 patients. Magnetic resonance imaging demonstrated mild cortical atrophy with widening of the extracerebral space and ventricles in all but one patient (Figs 1, 2). In 3 (patients 1, 2, and 8), previous neuroradiologic examinations did not indicate abnormal findings. In one patient (patient 9), neuroradiologic abnormalities were not observed throughout the clinical course.

Single-photon emission tomography was performed during the subacute or late phase in 5 patients. Four patients manifested marked hypoperfusion in the bilateral frontal areas (Fig 1), and one exhibited marked hypoperfusion in the left temporo-parieto-occipital area (Fig 2).

Electroencephalogram Findings

Electroencephalograms were recorded during the acute phase in 7 patients. Marked, generalized slowing was observed in 3 patients (patients 1, 5, and 9), and a slow basic rhythm in 1 patient (patient 3). However, electroencephalogram findings were unremarkable in 3 patients (patients 2, 6, and 8). An electroencephalogram during the subacute phase was performed in 8 patients, and revealed various degrees of abnormalities in all of them. Marked, generalized slowing was seen in 1 (patient 2), mild generalized slowing in 4 (patients 1, 3, 7, and 8), regional slowing in 2 (patients 5 and 6), and a slow basic rhythm in 1 (patient 4). Electroencephalograms during the late phase were performed in 6 patients (patients 1-6). Abnormalities in background activities were recognized in all of them, and paroxysmal discharges were observed in 3 (patients 3-5).

Treatments and Outcomes

Methylprednisolone pulse therapy was performed in 1 patient, intravenous dexamethasone therapy in 1, intravenous immunoglobulin therapy in 3, glycerol therapy in 3, and mannitol therapy in 1. In regard to anticonvulsants, diazepam was used in 6 patients, phenobarbital in 5, phenytoin in 2, carbamazepine in 2, valproate in 1, clonazepam in 1, and midazolam in 1. Mechanical ventilation was not necessary in any patients.

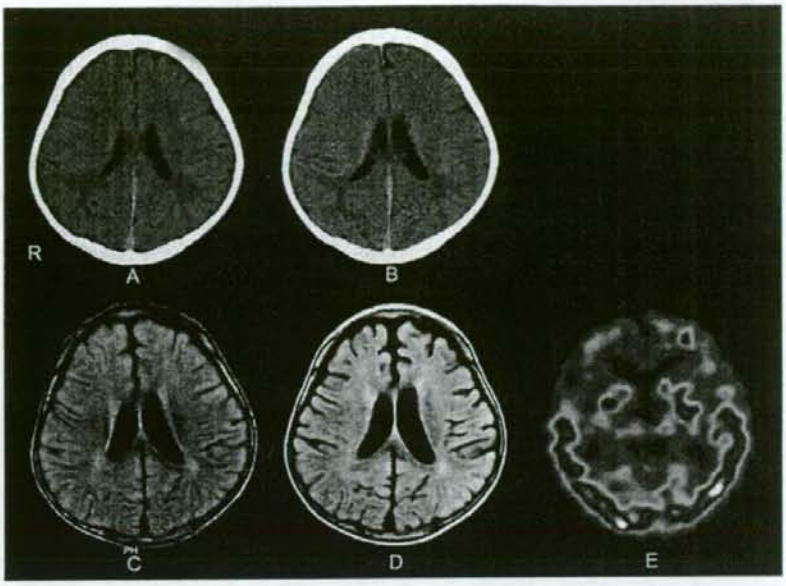

Figure 1. Neuroradiologic findings of patient 5. (A) Computed tomography on day of onset. No abnormal findings were recognized. (B) Computed tomography 5 days after onset. Mild blurring of gray-white matter differentiation was observed in the bilateral frontal areas. (C) Magnetic resonance imaging 14 days after onset (fluid-attenuated inversion recovery images, fast spin-echo, TR/TE/TI = 8000/120/1900 ms). Mild high intensities in the subcortical white matter were seen in the bilateral frontal areas. (D) Magnetic resonance imaging 39 days after onset (fluid-attenuated inversion recovery images, fast spin-echo, TR/TE/TI = 8000/120/2300 ms). Mild but diffuse cortical atrophy was observed. (E) Single-photon emission tomography 13 days after onset. Marked hypoperfusion was observed in the bilateral frontal areas.

The outcomes of patients are given in Table 1. No patients died, although all but one patient had various degrees of neurologic sequelae. Cognitive impairment was seen in 7 patients (severe in 3 patients, moderate in 3, and mild in 1), and motor impairment was seen in 7 (moderate in 1 patient, and mild in 6). In most patients, cognitive impairment was more prominent than motor impairment. The patient who had manifested mild cognitive impairment before the onset of encephalopathy (patient 4) had severe cognitive impairment with moderate motor impairment. The relationship between treatment and outcome could not be analyzed, because of the small number of patients and wide variety of treatments.

Discussion

Several authors proposed different names for acute encephalopathy syndromes with a relatively slow worsening of neurologic signs [6-13]. Although minor features are different among these syndromes, they have many points in common. Therefore, acute encephalopathy syndromes with a delayed worsening of consciousness should be integrated into one syndrome to avoid unnecessary confusion. To this end, we used the term "subacute" encephalopathy as a clinical entity to cover these syndromes, rather than devise a new name.

In the present study, we described the unique features of subacute encephalopathy. At the onset of encephalopathy, a prolonged or brief seizure was commonly observed, but some patients did not have a seizure at onset. The severity of decreased consciousness was invariably mild on the following day. Thereafter, worsening of consciousness began, and reached maximal severity 3-7 days after onset. Although neuroimaging was unremarkable at the outset, mild cortical atrophy was observed in most patients during the late phase. Most patients had moderate to severe

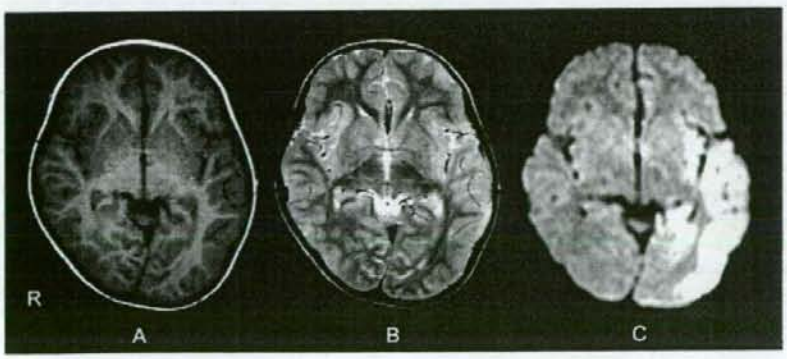

Figure 2. Neuroradiologic findings of patient 6: magnetic resonance imaging 9 days after onset. Subtle thickening of the cortex in the left temporo-parieto-occipital area was seen on T_1-weighted (A: fast spin-echo, TR/TE = 596/15 ms) and T_2-weighted (B, fast spin-echo, TR/TE = 4162/100 ms) images. Diffusion-weighted images (C: spin-echo echo-planar imaging, TR/TE = 2835/89 ms, b = 1000 sec/mm^2) demonstrated marked high intensities in the same region.

cognitive impairment, whereas motor impairment was relatively mild. Although these features are similar to those in previous reports [6-13], there are some differences between the patients in previous studies and ours.

One important difference involves the initial neurologic signs. A prolonged seizure or status epilepticus as the initial neurologic sign had been emphasized in this type of encephalopathy [5,10,12]. Yamanouchi and Mizuguchi included the presence of convulsive status epilepticus in the tentative diagnostic criteria of acute infantile encephalopathy predominantly affecting the frontal lobes [13]. However, a prolonged seizure was observed at the onset in only 3 of 9 patients in our cohort. Therefore, we think that the presence of a prolonged seizure or convulsive status epilepticus should not be stressed too strongly, although it is certainly an important neurologic sign at the onset.

Another prominent difference involves the localization of brain lesions. In previous studies, magnetic resonance imaging invariably revealed the involvement of the frontal lobes. Although this was the case in most of our patients, one of them (patient 6) exhibited a unilateral temporo-parieto-occipital lesion. In this patient, regional cerebral blood flow in the frontal lobes was not decreased. The localization of brain lesions will not be limited to the frontal lobes in patients with subacute encephalopathy. Age at onset was also different between our patients and those in previous studies. In previous studies, the age of patients was $\leq$3 years [9,12,13]. On the other hand, 6 of 9 patients were aged >36 months in this study. This finding indicates that subacute encephalopathy can be present in older children as well as in infants and young children.

The most important similarity between our study and previous studies involves poor neurologic outcomes despite a relatively mild loss of consciousness during the early phase. Although no patients were comatose on the next day after onset, moderate to severe cognitive impairment was present as a neurologic sequel in the majority of our patients. This was also the case with patients in previous studies [6-8,10-13]. We consider this to be the most prominent feature of subacute encephalopathy. We must be aware of the presence of this unique type of encephalopathy.

The pathophysiology of subacute encephalopathy remains unknown. Hypoxic brain injury is unlikely, because no patients had overt evidence of profound hypoxia. There have been several studies on the role of cytokines in the development of acute encephalopathy [14-17]. However, the role of cytokines in subacute encephalopathy is uncertain. Serum and cerebrospinal fluid levels of interleukin-6 were lower in patients with acute infantile encephalopathy predominantly affecting the frontal lobes than in patients with influenza-associated encephalopathy. A relatively slow worsening of neurologic signs may be suggestive of delayed neuronal loss caused by prolonged convulsions. Takanashi et al. suggested an accumulation of glutamate because of hyperactivity of glutamatergic neurons, using magnetic resonance spectroscopy in a child with prolonged febrile seizure with encephalopathy [5]. Apoptotic changes were also revealed in patients with acute encephalopathy [18]. However, these findings have not been investigated in children with subacute encephalopathy. Further multidisciplinary studies are necessary to clarify the pathogenesis of subacute encephalopathy.

The diagnostic value of neuroimaging in subacute encephalopathy remains unclear at present. Computed tomography or magnetic resonance imaging within a few days after the onset will be useless. Takanashi et al. indicated that magnetic resonance imaging within 2 days of the onset of encephalopathy revealed no acute lesions in children with prolonged febrile seizures with encephalopathy [5]. Computed tomography or conventional magnetic resonance imaging during the subacute phase will be of limited use. Computed tomography may reveal a blurring of gray-white matter differentiation, and magnetic resonance imaging may demonstrate mildly increased intensities in the subcortical white matter on T_2-weighted and fluid-attenuated inversion-recovery images. However, these changes can be subtle and overlooked. Diffusion-weighted imaging will be useful if it is performed during an appropriate period, as stated in previous studies [5,10,12].

The early diagnosis of subacute encephalopathy is of clinical interest. However, no useful clues have been delineated for such an early diagnosis. Neuroimaging during the early phase will not be useful, as explained above. Laboratory data will not be helpful, because the abnormalities in laboratory data are non-specific and are not pathogomotic in children with subacute encephalopathy. We think that electroencephalograms may be useful in some patients, because electroencephalograms indicated abnormalities in 4 of 7 patients in whom they were performed during the acute phase. Yamanouchi et al. reported that electroencephalograms were recorded at onset in 6 of 9 patients with acute infantile encephalopathy predominantly affecting the frontal lobes, and revealed slow background activity [12]. We think that careful evaluation of consciousness will be also useful for early recognition of subacute encephalopathy. Maegaki et al. reported on acute encephalopathy with a biphasic clinical course, whose clinical features were very similar to those of subacute encephalopathy, in 6 of 16 patients with grade II or III loss of consciousness according to the Japan Coma Scale, 12 hours after onset [8]. Therefore, a combination of electroencephalograms and a precise neurologic examination focusing on responsiveness and wakefulness will be a diagnostic clue in regard to subacute encephalopathy.

In conclusion, "subacute" encephalopathy, characterized by a delayed worsening of neurologic signs, is a distinct subtype of acute encephalopathy. Early recognition is not easy, because the initial neurologic signs are varied, and laboratory data and neuroimaging are unremarkable during the acute phase. Magnetic resonance imaging during the late phase reveals mild cortical atrophy, and single-photon emission tomography indicates hypoperfusion

in the affected regions. The neurologic outcome is poor in most patients. Recognition of subacute encephalopathy is important, and a method to promote early diagnosis is desirable.

This work was supported by grant 17209037 from the Ministry of Education, Culture, Sports, Science and Technology of Japan. For their collaboration in this study, we thank Motomasa Suzuki, MD, Toru Kato, MD, Fumio Hayakawa, MD, PhD, Tomohiko Nakata, MD, Ayako Sofue, MD, PhD, Takeshi Tsuji, MD, Hirokazu Kurahashi, MD, Taketo Ikuta, MD, Hiroko Kakizawa, MD, PhD, Teruyoshi Azuma, MD, Yoshiko Suzuki, MD, PhD, and Tatsuya Fukazawa, MD.

References

[1] **Mizuguchi** M. Acute necrotizing encephalopathy of childhood: A novel form of acute encephalopathy prevalent in Japan and Taiwan. Brain Dev 1997;19:81-92.

[2] **Okumura** A, Noda E, Ikuta T, et al. Transient encephalopathy with reversible white matter lesions in children. Neuropediatrics 2006; 37:159-62.

[3] **Tada** H, Takanashi J, Barkovich AJ, et al. Clinically mild encephalitis/encephalopathy with a reversible splenial lesion. Neurology 2004;63:1854-8.

[4] **Takanashi** J, Barkovich AJ, Shiihara T, et al. Widening spectrum of a reversible splenial lesion with transiently reduced diffusion. AJNR 2006;27:836-8.

[5] **Takanashi** J, Oba H, Barkovich AJ, et al. Diffusion MRI abnormalities after prolonged febrile seizures with encephalopathy. Neurology 2006;66:1304-9.

[6] **Itomi** K, Okumura A, Kato T, et al. Subacute encephalitis/encephalopathy with residual cognitive deficit [in Japanese]. No To Hattatsu 2005;37:467-72.

[7] **Maegaki** Y, Kondo A, Okamoto R, et al. Clinical characteristics of acute encephalopathy of obscure origin: A biphasic clinical course is a common feature. Neuropediatrics 2006;37:269-77.

[8] **Maegaki** Y, Kurosawa Y, Hayashi A, et al. An early diagnosis of acute encephalopathy using early clinical, laboratory, and neuroimaging findings [in Japanese]. J Jpn Pediatr Soc 2006;110: 1550-7.

[9] **Nagasawa** T, Kimura I, Abe Y, Oka A. HHV-6 encephalopathy with cluster of convulsions during eruptive stage. Pediatr Neurol 2007; 36:61-3.

[10] **Okamoto** R, Fujii S, Inoue T, et al. Biphasic clinical course and early white matter abnormalities may be indicators of neurological sequelae after status epilepticus in children. Neuropediatrics 2006;37: 32-41.

[11] **Sato** S, Kumada S, Koji T, Okaniwa M. Reversible frontal lobe syndrome associated with influenza virus infection in children. Pediatr Neurol 2000;22:318-21.

[12] **Yamanouchi** H, Kawaguchi N, Mori M, et al. Acute infantile encephalopathy predominantly affecting the frontal lobes. Pediatr Neurol 2006;34:93-100.

[13] **Yamanouchi** H, Mizuguchi M. Acute infantile encephalopathy predominantly affecting the frontal lobes (AIEF): A novel clinical category and its tentative diagnostic criteria. Epilepsy Res 2006;70 (Suppl. 1):S263-8.

[14] **Aiba** H, Mochizuki M, Kimura M, Hojo H. Predictive value of serum interleukin-6 level in influenza virus-associated encephalopathy. Neurology 2001;57:295-9.

[15] **Hosoya** M, Nunoi H, Aoyama M, Kawasaki Y, Suzuki H. Cytochrome C and tumor necrosis factor-alpha values in serum and cerebrospinal fluid of patients with influenza-associated encephalopathy. Pediatr Infect Dis J 2005;24:467-70.

[16] **Ichiyama** T, Morishima T, Isumi H, Matyubara T, Furukawa S. Analysis of cytokine levels and NF-kappaB activation in peripheral blood mononuclear cells in influenza virus-associated encephalopathy. Cytokine 2004;27:31-7.

[17] **Kawada** J, Kimura H, Ito Y, et al. Systemic cytokine responses in patients with influenza-associated encephalopathy. J Infect Dis 2003;188:690-8.

[18] **Nakai** Y, Itoh M, Mizuguchi M, et al. Apoptosis and microglial activation in influenza encephalopathy. Acta Neuropathol (Berl) 2003; 105:223-9.

Comparison of Quantitative EEGs Between Parkinson Disease and Age-Adjusted Normal Controls

Kan Serizawa, Satoshi Kamei,* Akihiko Morita,* Motohiko Hara,* Tomohiko Mizutani,* Hirokazu Yoshihashi,* Mai Yamaguchi,* Jun Takeshita,* and Kaname Hirayanagi†*

Summary: Quantitative EEG (qEEG) findings in Parkinson disease (PD) have been reported in only five previous studies. In these studies, the sample size was small and the distribution of qEEG changes was not estimated. This is the first qEEG evaluation not only employing multiple logistic regression analysis but also estimating the distribution of qEEG changes. The subjects comprised 45 PD patients without remarkable dementia and 40 age-adjusted normal controls. The lack of ischemic lesions in all subjects was confirmed by MRI. Absolute power values were measured for four frequency bands from delta to beta. The electrodes were divided into six, viz. frontal pole, frontal, central, parietal, temporal, and occipital locations. We calculated the spectral ratio, i.e., the sum of the power values in the alpha and beta waves divided by the sum of the values in the slow waves. The dependent variable was either PD or normal control; the independent variables were the spectral ratios, age, sex, and Mini-Mental State Examination score. The significant predictive variables in PD were the spectral ratios at all electrode locations except for the frontal pole (frontal location: $P = 0.025$, other locations: $P < 0.01$). PD presented diffuse slowing in the qEEG when compared with age-adjusted normal controls.

Key Words: Parkinson disease, Quantitative EEG, Multiple logistic regression analysis, Electrode distribution, Ischemia.

(*J Clin Neurophysiol* 2008;25: 361–366)

Diffuse or localized slowing of the EEG in patients with Parkinson disease (PD), as evaluated by visual inspection, has been described (Neufeld et al., 1988; Yeager et al., 1966). However, comparisons of quantitative EEG (qEEG) analysis between PD patients and "age-adjusted normal controls" (CTRL) subjects have been reported in only five studies (Neufeld et al., 1994; Pezard et al., 2001; Primavera et al., 1992; Soikkeli et al., 1991; Tanaka et al., 2000). The sample sizes in these earlier qEEG studies were limited to 30 or below. The distribution of electrode locations for the qEEG findings in PD was also not evaluated in these previous studies. Moreover, although the PD was well recognized as a geriatric disease, the estimation of intracerebral ischemic lesions in the subjects was made in the only one previous study (Tanaka et al., 2000). The present study provides the first evaluation of the difference in qEEG findings using multiple logistic regression analysis, by comparing 45 PD patients and 40 CTRL subjects after confirmation of the absence of intracerebral ischemic lesions by cranial MRI, and also provides the first evaluation of the distribution of qEEG electrode locations in PD.

PATIENTS AND METHODS

Patient and Control Definitions

At the outset of the present study, PD patients without remarkable dementia were defined as being those with sporadic PD who revealed a score of 24 or more points on the Mini-Mental State Examination (MMSE) based on the *Diagnostic and Statistical Manual of mental disorders, 4th ed.* (DSM-IV) criteria for dementia in accordance with a previously reported study (Burn et al., 2006). All patients were scanned for T1-, T2-weighted images, fluid-attenuated inversion recovery (FLAIR) images, and diffusion images using a cranial MRI (1.5-T Siemens Magnetom Symphony, Munich, Germany). We also arbitrarily defined patients without any intracerebral ischemic changes including even only one asymptomatic lacuna or slight periventricular hyperintensity in accordance with the reported classification of periventricular hyperintensity (Fazekas et al., 1987) using T2 and FLAIR images.

The number of consecutive patients in this study after obtaining informed written consent was 125 of 158 who were diagnosed as sporadic form PD at the Neurology Clinic, Nihon University Itabashi Hospital, during the period from December 2004 to July 2006. The clinical diagnosis of sporadic PD was made according to the UK PD Brain Bank criteria (Gibb and Lees, 1988). On the basis of the clinical features and neuroradiological findings including brain com-

From the *Division of Neurology, Department of Medicine, Nihon University School of Medicine, Tokyo, Japan; and †Department of Hygiene and Public Health, Nihon University of Physical Education, Tokyo, Japan.

K. Hirayanagi performed the statistical analysis.

This work was supported by a grant from the Ministry of Education, Culture, Sports, Science, and Technology of Japan for the promotion of industry-university collaboration at Nihon University, Japan, a Grant for an "Academic Frontier" Project for Private Universities (Matching fund subsidy from MEXT), and Grants-in-Aid from the Research Committee of CNS Degenerative Diseases, the Ministry of Health, Labor and Welfare of Japan.

Address correspondence and reprint requests to Satoshi Kamei, M.D., Division of Neurology, Department of Medicine, Nihon University School of Medicine, 30-1 Oyaguchi-kamimachi, Itabashi-ku, Tokyo 173-8610, Japan; e-mail: skamei@med.nihon-u.ac.jp.

Copyright © 2008 by the American Clinical Neurophysiology Society

ISSN: 0736-0258/08/2506-0361

puted tomography (CT) and MRI at the time of more than 12 months after onset, we excluded other forms of parkinsonism which included (1) dementia with Lewy bodies (DLB) (Geser et al., 2005; McKeith et al., 1996), (2) drug-induced parkinsonism, (3) vascular parkinsonism, and (4) atypical parkinsonism with absent or minimal responses to antiparkinsonian drugs. One of us (S.K.) diagnosed 119 of the 125 patients as having sporadic PD, and excluded the remaining six patients from the present study, because of the possibility of vascular parkinsonism in four patients and of DLB in two patients. According to the above-mentioned MRI criteria for intracerebral ischemic lesions, 71 of the 119 patients were confirmed as sporadic PD patients without intracerebral ischemic lesions. Moreover, 45 of these 71 patients satisfied the above-mentioned criteria for lack of remarkable dementia and no anticholinergic drug administration which might influence the qEEG findings. These PD patients thus had a good response to antiparkinsonian drugs and did not have a history of visual hallucinations or a fluctuating cognitive ability suggestive of a clinical diagnosis of DLB at the time of more than 12 months after their onset. These 45 PD patients were therefore enrolled on the present study.

The CTRL subjects were also defined as patients without any organic intracerebral disease who were 60 or more years old and exhibited no intracerebral ischemic lesions on cranial MRI. In total, 102 outpatients were diagnosed as having nonintracerebral diseases based on neurologic examinations, EEG, and cranial MRI at the Neurology Clinic during the same period as that mentioned above for PD. Of these 102 patients, 62 were confirmed to have no intracerebral ischemic lesions by MRI, and 40 of these 62 patients provided us with informed written consent and were enrolled as the CTRL subjects for the present study. The clinical diagnosis in these 40 patients consisted of cervical spondylosis (18 patients), lumbar spondylosis (7 patients), tension-type headache (6 patients), aural vertigo (4 patients), benign paroxysmal positional vertigo (3 patients), carpal tunnel syndrome (1 patient), and intercostal neuralgia (1 patient). None of the 40 normal control subjects was taking centrally active drugs at the time of EEG examination.

Informed written consent in the present study was obtained from each subject according to a protocol approved by the Ethic Committee for Human Studies at Nihon University Itabashi Hospital.

Assessments

The EEG recordings and qEEG analysis used in the present study were as described previously (Kamei et al., 1999, 2005). Briefly, the EEG in each subject was obtained in the resting awake condition with the eyes closed. The EEG was recorded on a magnetic optical disk from 16 electrode locations according to the 10–20 international system using a digital EEG instrument (Neurofax EEG-1100, Nihon Kohden, Tokyo, Japan). The EEG was referenced to the ipsilateral earlobes. A minimum 60 seconds of qEEG data were selected visually by an EEG analyst (K.S.), from each subject and digitized at 200 Hz with a time constant of 0.3 seconds, employing a high-frequency filter of 60.0 Hz. Thirty or more epochs with a duration of 2.56 seconds were thus collected from the subsequent resting period at the time of closed eyes for analysis of the qEEG. The analytical procedure involved application of fast Fourier transformation of the collected EEG signals with a frequency analyzer (QP-220A, Nihon Kohden, Tokyo, Japan). The frequency ranges were divided into four bands, as follows: delta (1.17–3.91 Hz), theta (4.30–7.81 Hz), alpha (8.20–12.89 Hz), and beta (13.28–30.08 Hz). The absolute powers of each frequency band were calculated at each electrode location in each subject. The absolute power value was obtained by integrating the appropriate part of the spectrum.

Statistical Analysis

SPSS software version 12.0 (SPSS Inc., Chicago, IL) was used for the statistical analysis. At the end of December 2006, the statistical analyst (K.H.) at another independent institute collected the data for the clinical parameters from S.K. and those for the qEEG from K.S. Shapiro-Wilk test was used to evaluate whether the continuous variable data showed a normal distribution or not. The parametric analysis was applied to a normal data, otherwise the nonparametric analysis was applied to a non-normal data. Differences of clinical features between the PD and CTRL were used by the Fisher's probability test and Mann-Whitney U test. The differences between the right and left cerebral absolute power values in the subjects were evaluated by Wilcoxon signed-rank test. There were no significant differences in absolute power values between the right- and left-sided locations in the PD patients ($P = 0.656$) or CTRL subjects ($P = 0.925$). The present study was thus based on an analysis of the combined data for the absolute power values in the right and left-sided electrode locations. The electrodes were divided into six locations as follows: frontal pole (Fp: Fp_1 and Fp_2), frontal (F: F_3, F_4, F_7, and F_8), central (C: C_3 and C_4), parietal (P: P_3 and P_4), temporal (T: T_3, T_4, T_5, and T_6), and occipital (O: O_1 and O_2) locations.

For evaluation of the slowing of the qEEG in the present study, the spectral ratio was calculated by the same mode of analysis as in a previously reported assessment of EEG slowing in Alzheimer disease (Lindau et al., 2003). The "spectral ratio" is the ratio of the sum of the absolute powers in the alpha and fast frequency bands divided by the sum of the absolute powers in the delta and theta frequency bands. The differences of the spectral ratios among each electrode location in the CTRL and PD were first estimated by the Friedman's test and then the *post hoc* test was applied by the Wilcoxon singed-rank test with Bonferroni correction.

Differences in qEEG findings at each electrode location between the PD and CTRL were evaluated by multiple logistic regression analysis. A dichotomous dependent (Y) variable was assigned with a value of 1 for PD, and with that of 0 for CTRL. The independent variables (X) were categorized as (1) sex (male = 1, female = 0), (2) patient's age at this assessment (years; real number), (3) MMSE (score; real number), and (4) spectral ratio (real number). Moreover, backward stepwise logistic regression analysis using maximum likelihood estimation (Y = PD vs. CTRL subjects, X = 6 electrode locations) was used to detect the best predictor of the electrode location in terms of the spectral ratio for PD.

Copyright © 2008 by the American Clinical Neurophysiology Society

The level of statistical significance for this study was defined as 0.05.

RESULTS

The clinical features of the PD and CTRL enrolled in the present study were summarized in Table 1. The differences in sex, age at the assessment, and score on the MMSE between the PD patients and CTRL subjects were not statistically significant. The Hoehn and Yahr stages in 45 PD patients were as follows: 1 patient (2.2%) of stage I, 17 patients (37.8%) of stage II, 22 patients (48.9%) of stage III, and 5 patients (11.1%) of stage IV. These PD patients were treated with the following agents: levodopa in 36 patients (80.0%), dopamine agonists in 36 patients (80.0%), amantadine in 12 patients (26.7%), monoamine oxidase inhibitor in 10 patients (22.2%), L-threo-3,4-dihydroxyphenylserine in 6 patients (13.3%), and no medication in 2 patients (4.4%).

The ratios of the absolute power values in each frequency band and at each electrode location to the total absolute power values in the 45 PD patients were shown in Table 2, and those in the 40 CTRL subjects in Table 3. The ratios in the slow waves against the total power value in PD were higher, and those in the alpha or fast waves were lower than those in the CTRL at all electrode locations. The results for the differences of spectral ratio among each electrode location in PD and CTRL were statistically significant in both groups ($P < 0.0001$ in both). The post hoc test for the significant difference among each of the electrode locations were as following electrode locations; Fp versus F, Fp versus C, Fp versus P, Fp versus T, Fp versus O, F versus C, F versus P, F versus T, and F versus O in CTRL ($P < 0.001$ in these locations) and Fp versus C, Fp versus P, Fp versus T, and Fp versus O in PD ($P < 0.001$ in these locations).

The results of the single and multiple logistic regression analyses for the predictor of PD against CTRL were summarized in Table 4. The significant independent variables of the PD using multiple logistic regression analysis were only the spectral ratios at all electrode locations except for Fp. The spectral ratio at the O electrode location was the best predictor of PD (Odds ratio = 0.648, $P = 0.016$).

DISCUSSION

There have been two previous studies on EEG slowing based on visual estimations in large numbers of patients with PD (Neufeld et al., 1988; Yeager et al., 1966). Yeager et al. (1966) reported that 36.3% of 223 patients with PD exhibited abnormal findings on EEG, which consisted of diffuse slowing, localized slowing, or both. Neufeld et al. (1988) also

TABLE 1. Clinical Features of the Studied Patients With PD and CTRL Subjects

	PD Patients Without Remarkable Dementia (A)	CTRL Subjects (B)	Comparison Between (A) and (B)
Number of patients	45	40	
Sex: male, n'(%)	22 (48.9)	14 (35.0)	NS*
Age at assessment (years) (minimum, mean, median, and maximum)	61, 71.4, 71, 87	60, 69.2, 68, 82	NS†
Duration from onset (months) (minimum, mean, median, and maximum)	12, 67.8, 60, 192		
Mini-Mental State Examination (minimum, mean, median, and maximum)	24, 26.9, 27, 30	24, 27.0, 27, 30	NS‡

*$P = 0.272$; Fisher exact test probability test.
†$P = 0.06$; Mann-Whitney U test.
‡$P = 0.986$; Mann-Whitney U test.
PD, Parkinson disease; CTRL, age-adjusted normal control; NS, not significant.

TABLE 2. Ratio of Absolute Power Values at Each Frequency Band and Electrode Location Against Total Power Value in 45 Patients With PD

Frequency Band	Electrode Location																	
	Fp			F			C			P			T			O		
	M	SE	%*	M	SE	%*	M	SE	%*	M	SE	%*	M	SE	%*	M	SE	%*
Delta	0.061	0.008	37	0.074	0.006	30	0.040	0.004	27	0.035	0.003	25	0.045	0.004	25	0.032	0.003	24
Theta	0.044	0.003	30	0.078	0.005	31	0.045	0.003	32	0.044	0.004	31	0.057	0.005	32	0.044	0.005	31
Alpha	0.042	0.004	30	0.084	0.007	33	0.053	0.004	37	0.056	0.005	39	0.064	0.005	37	0.059	0.007	41
Beta	0.006	0.0006	4	0.011	0.001	5	0.007	0.0006	5	0.006	0.0005	5	0.009	0.0008	5	0.005	0.0004	4
Sum of ratios at each electrode location	0.153	0.009	100	0.247	0.007	100	0.145	0.004	100	0.141	0.005	100	0.175	0.005	100	0.140	0.007	100

*Percentage of absolute power value in each frequency band against sum of power values at each electrode location.
PD, Parkinson disease; M, mean value; SE, standard error; FP, frontal pole; F, frontal; C, central; P, parietal; T, temporal; O, occipital location.

Copyright © 2008 by the American Clinical Neurophysiology Society

TABLE 3. Ratio of Absolute Power Values at Each Frequency Band and Electrode Location Against Total Power Value in 40 CTRL Subjects

Frequency Band	Electrode Location																	
	Fp			F			C			P			T			O		
	M	SE	%*	M	SE	%*	M	SE	%*	M	SE	%*	M	SE	%*	M	SE	%*
Delta	0.062	0.009	37	0.060	0.005	27	0.031	0.003	22	0.029	0.002	19	0.037	0.003	22	0.024	0.003	17
Theta	0.033	0.003	23	0.054	0.006	24	0.031	0.003	22	0.029	0.003	20	0.036	0.004	21	0.027	0.003	19
Alpha	0.045	0.004	34	0.094	0.008	42	0.068	0.005	48	0.085	0.007	53	0.083	0.005	50	0.107	0.011	59
Beta	0.008	0.0009	6	0.016	0.002	7	0.010	0.001	8	0.011	0.001	7	0.012	0.001	7	0.009	0.001	5
Sum of ratios at each electrode location	0.148	0.011	100	0.224	0.009	100	0.140	0.005	100	0.154	0.006	100	0.168	0.005	100	0.167	0.012	100

*Percentage of absolute power value in each frequency band against sum of power values at each electrode location.
CTRL, age-adjusted normal control; M, mean value; SE, standard error; FP, frontal pole; F, frontal; C, central; P, parietal; T, temporal; O, occipital location.

TABLE 4. Results of Single and Multiple Logistic Regression Analyses for the Predictor of PD Patients Against CTRL Subjects at Each Electrode Location

Electrode Location	Variable	Single Logistic Regression Analysis		Multiple logistic Regression Analysis	
		Odds ratio (95% CI)	*P*	Odds ratio (95% CI)	*P*
Fp	Spectral ratio[a]	0.727 (0.441–1.198)	0.211	0.771 (0.458–1.298)	0.328
	Age (real number)	1.067 (0.991–1.149)	0.087	1.060 (0.980–1.146)	0.145
	Sex (m = 1, f = 0)	1.776 (0.741–4.257)	0.198	1.349 (0.499–3.650)	0.555
	MMSE (real number)	0.991 (0.814–1.206)	0.929	1.044 (0.842–1.296)	0.694
F	Spectral ratio[a]	0.446 (0.236–0.842)	0.013*	0.474 (0.247–0.911)	0.025*
	Age (real number)	Same values as those in the Fp columns[b]		1.052 (0.971–1.140)	0.217
	Sex (m = 1, f = 0)	Same values as those in the Fp columns[b]		1.286 (0.468–3.539)	0.626
	MMSE (real number)	Same values as those in the Fp columns[b]		1.040 (0.834–1.300)	0.730
C	Spectral ratio[a]	0.405 (0.222–0.738)	0.003*	0.422 (0.228–0.781)	0.006*
	Age (real number)	Same values as those in the Fp columns[b]		1.045 (0.962–1.136)	0.230
	Sex (m = 1, f = 0)	Same values as those in the Fp columns[b]		1.301 (0.461–3.670)	0.620
	MMSE (real number)	Same values as those in the Fp columns[b]		1.013 (0.809–1.271)	0.904
P	Spectral ratio[a]	0.470 (0.292–0.758)	0.002*	0.483 (0.297–0.787)	0.003*
	Age (real number)	Same values as those in the Fp columns[b]		1.057 (0.971–1.151)	0.200
	Sex (m = 1, f = 0)	Same values as those in the Fp columns[b]		1.220 (0.423–3.519)	0.713
	MMSE (real number)	Same values as those in the Fp columns[b]		1.035 (0.821–1.305)	0.769
T	Spectral ratio[a]	0.386 (0.209–0.712)	0.002*	0.402 (0.218–0.744)	0.004*
	Age (real number)	Same values as those in the Fp columns[b]		1.059 (0.974–1.151)	0.182
	Sex (m = 1, f = 0)	Same values as those in the Fp columns[b]		1.010 (0.384–3.129)	0.864
	MMSE (real number)	Same values as those in the Fp columns[b]		1.067 (0.846–1.347)	0.585
O	Spectral ratio[a]	0.569 (0.409–0.792)	0.0008*	0.577 (0.413–0.805)	0.001*
	Age (real number)	Same values as those in the Fp columns[b]		1.065 (0.978–1.160)	0.165
	Sex (m = 1, f = 0)	Same values as those in the Fp columns[b]		0.986 (0.345–2.950)	0.986
	MMSE (real number)	Same values as those in the Fp columns[b]		1.050 (0.828–1.331)	0.686

*Statistically significant ($P < 0.05$).
[a]Spectral ratio is sum of absolute power values in the alpha and beta waves divided by sum of absolute power values in the delta and theta waves.
[b]Since the studied PD patients and the normal controls were the same subjects for all electrode locations, the results of the single logistic regression analysis for age and sex were uniform.
PD, Parkinson disease; CTRL, age-adjusted normal control; MMSE, Mini-Mental State Examination; FP, frontal pole; F, frontal; C, central; P, parietal; T, temporal; O, occipital location; m, male; f, female; CI, confidence interval.

found that a mild slowing on EEG was present in 34% of 128 patients with PD. Since EEG findings become altered in aged people (Van Sweden et al., 1999), it is considered necessary that EEG evaluations in PD should be compared with aged control subjects. However, the above two previous reports evaluated only the PD patients without comparisons with aged control subjects. On the other hand, the five previous investigations of qEEG in PD (Neufeld et al., 1994; Pezard

Copyright © 2008 by the American Clinical Neurophysiology Society

TABLE 5. Profiles of Previous qEEG Studies Comparing PD and CTRL Subjects

Authors (Published Year)	Sample Numbers		Estimation of Intracerebral Ischemic Lesions in Each Subject Using MRI	Parameter of Evaluation	Statistical Evaluation for Comparisons Between PD and CTRL	Statistical Evaluation at Each Electrode Location	Statistical Significance of Results Between PD and CTRL
	PD	CTRL					
Soikkeli et al. (1991)	18	20	ND	Relative amplitude	1-way ANOVA	NE	S
Primavera and Novello (1992)	30	30	ND	Percent difference	Wilcoxon signed ranks test	NE	S
Neufeld et al. (1994)	10	10	ND	Relative amplitude	2-way ANOVA	NE	NS
Tanaka et al. (2000)	29	11	Estimated	Absolute power value	ANOVA	NE	S
Pezard et al. (2001)	9	9	ND	Relative power value <Non-linear EEG analysis>	ANOVA	NE	S
Serizawa et al. (Present study)	45	40	Estimated	Spectral ratio	Multiple logistic regression analysis	Examined	S

qEEG, quantitative electroencephalogram; PD, Parkinson disease; CTRL, age-adjusted normal control; MRI, magnetic resonance imaging; ND, not done; NE, not examined; S, statistically significant ($P < 0.05$); NS, not significant ($P \geq 0.05$); ANOVA, analysis of variance.

et al., 2001; Primavera and Novello, 1992; Soikkeli et al., 1991; Tanaka et al., 2000) did undertake evaluations based on a comparison with aged control subjects. Details of these five qEEG studies were summarized in Table 5. Since EEG slowing was also reported in patients with vascular parkinsonism (Zijlmans et al., 1998), it was assumed that intracerebral ischemic lesions might influence the qEEG findings if our examined subjects had ischemic lesions. We therefore considered it necessary to estimate the intracerebral ischemic lesions when evaluating the difference in qEEG between PD and CTRL. Based on the inclusion criterion of an absence of intracerebral ischemic lesions in the present study, we selected 45 of 119 sporadic PD patients and 40 of 102 CTRLs to supply the data used in this comparative investigation. There was only one previous study (Tanaka et al., 2000) undertaking an evaluation of the EEG in PD who was assessed for intracerebral ischemic lesions using MRI.

Among the five previous investigations of qEEG in PD, Soikkeli et al. (1991), Primavera and Novello (1992), and Tanaka et al. (2000) found that slowing of the qEEG was significant and remarkable in PD. Pezard et al. (2001) also noted that the relative power value of the beta wave in PD was significantly decreased when compared with that in CTRL. However, Neufeld et al. (1994) reported that no significant difference was evident between the two groups. Pezard et al. (2001) undertook evaluations of EEG alterations in PD by nonlinear EEG analysis, which represented a new method of EEG analysis at that time, and found that PD showed brain dysfunction when compared with CTRL. However, since new parameters such as entropy and slope asymmetry were adopted in their study, it was unknown how such dysfunction was reflected in terms of frequency changes on conventional EEG. The present study of qEEG between 45 PD patients and 40 CTRL subjects demonstrated that the PD revealed a significant slowing on their EEG when compared with the CTRL.

Furthermore, a statistical evaluation at each electrode location was not undertaken in these five previous investigations (Neufeld et al., 1994; Pezard et al., 2001; Primavera and Novello, 1992; Soikkeli et al., 1991; Tanaka et al., 2000). Neufeld et al. (1994) provided detailed data on the relative amplitude at each electrode location; however, since the statistical results for both groups were not significantly different, evaluations at each electrode location could not be made. Statistical evaluations in the remaining four previous investigations were performed on the basis of combined data for all electrode locations (Pezard et al., 2001; Primavera and Novello, 1992; Soikkeli et al., 1991; Tanaka et al., 2000). Thus, the present study using multiple logistic regression analysis is the first to reveal that slowing of EEG in PD can be detected at all electrode locations except for Fp.

According to the concept of Braak et al., (2004) of the progression in PD, the components of the autonomic, limbic, and somatomotor systems become damaged as the disease progresses. In stages 3 to 4 of that pathologic process, the substantia nigra and other nuclear grays of the midbrain and forebrain become the focus of initially slight and then severe pathologic changes. At this point, most individuals probably cross the threshold to the symptomatic phase of the illness. In stages 5 to 6, the pathologic process becomes distributed to the diffuse neocortex, and the disease manifests itself in all of its clinical dimensions. The diffuse slowing of the qEEG in PD patients observed in the present study was considered to be an appropriate finding in accordance with Braak's concept. Subtle cognitive deficits are almost universally identified even at the early stage of PD upon detailed neuropsychological testing (Lees and Smith, 1983). Community-based studies have suggested that 78% of patients with PD would

Copyright © 2008 by the American Clinical Neurophysiology Society

develop clinically defined dementia during an 8-year study period (Aarsland et al., 2003). A recent meta-analysis of prevalence carried out on dementia in PD has estimated that 31.5% of PD patients fulfill diagnostic criteria for dementia (Emre et al., 2007). In view of the lack of detailed neuropsychological tests and postmortem confirmation in the present study, some of the patients examined in our study would be expected to develop dementia. The diffuse slowing on the qEEG might thus reflect brain dysfunction before the development of clinically defined remarkable cognitive impairment. On the other hand, the reason for the findings indicating the spectral ratio at the O electrode location as the best predictor of PD and the lack of significant slowing at the Fp location in the present study could be related to the occipital dominant distribution of the alpha wave. In other words, it might be easy to demonstrate slowing of the qEEG at the O location, but hard to detect it at the Fp location. Thus, patients with PD are presented essentially diffuse slowing of their qEEG based on the pathologic changes occurring in PD.

In conclusion, the present study is the first qEEG evaluation not only using multiple logistic regression analysis but also estimating the distribution of the qEEG change. Based on the pathologic change in PD, PD significantly presented diffuse slowing of their qEEG when compared with CTRL.

ACKNOWLEDGMENTS

The authors are indebted to Professor Mitsuru Kawamura, MD, Department of Neurology, Showa University School of Medicine, Tokyo, Japan, and Dr. Xiangji Li, PhD, Division of Neurology, 1st Department of Engineering, Nihon Kohden Co., Tokyo, Japan, for their invaluable comments regarding this investigation.

REFERENCES

Aarsland D, Andersen K, Larsen JP, et al. Prevalence and characteristics of dementia in Parkinson disease: an 8-year prospective study. *Arch Neurol.* 2003;60:387–392.

Braak H, Ghebremedhin E, Rüb U, et al. Stages in the development of Parkinson's disease-related pathology. *Cell Tissue Res.* 2004;318:121–134.

Burn DJ, Rowan EN, Allan LM, et al. Motor subtype and cognitive decline in Parkinson's disease, Parkinson's disease with dementia and dementia with Lewy bodies. *J Neurol Neurosurg Psychiatry.* 2006;77:585–589.

Emre M, Aarsland D, Brown R, et al. Clinical diagnostic criteria for dementia associated with Parkinson's disease. *Mov Disord.* 2007;22:1689–1707.

Fazekas F, Chawluk JB, Alavi A, et al. MR signal abnormalities at 1.5 T in Alzheimer's dementia and normal aging. *Am J Roentgenol.* 1987;149:351–356.

Geser F, Wenning GK, Poewe W, et al. How to diagnose dementia with Lewy bodies: state of the art. *Mov Disord.* 2005;20(Suppl 12):S11–S20.

Gibb WR, Lees AJ. The relevance of the Lewy body to the pathogenesis of idiopathic Parkinson's disease. *J Neurol Neurosurg Psychiatry.* 1988;51:745–752.

Kamei S, Tanaka N, Matsuura M, et al. Blinded, prospective and serial evaluation by quantitative-EEG in interferon-alpha-treated hepatitis-C. *Acta Neurol Scand.* 1999;100:25–33.

Kamei S, Oga K, Matsuura M, et al. Correlation between quantitative-EEG alterations and age in patients with interferon-alpha-treated hepatitis C. *J Clin Neurophysiol.* 2005;22:49–52.

Lees AJ, Smith E. Cognitive deficits in the early stages of Parkinson's disease. *Brain.* 1983;106:257–270.

Lindau M, Jelic V, Johansson SE, et al. Quantitative EEG abnormalities and cognitive dysfunctions in frontotemporal dementia and Alzheimer's disease. *Dement Geriatr Cogn Disord.* 2003;15:106–114.

McKeith IG, Galasko D, Kosaka K, et al. Consensus guidelines for the clinical and pathologic diagnosis of dementia with Lewy bodies (DLB): report of the consortium on DLB international workshop. *Neurology.* 1996;47:1113–1124.

Neufeld MY, Inzelberg R, Korczyn AD EEG in demented and non-demented parkinsonian patients. *Acta Neurol Scand.* 1988;78:1–5.

Neufeld MY, Blumen S, Aitkin I, et al. EEG frequency analysis in demented and nondemented parkinsonian patients. *Dementia.* 1994;5:23–28.

Pezard L, Jech R, Ruzicka E. Investigation of non-linear properties of multichannel EEG in the early stages of Parkinson's disease. *Clin Neurophysiol.* 2001;112:38–45.

Primavera A, Novello P. Quantitative electroencephalography in Parkinson's disease, dementia, depression and normal aging. *Neuropsychobiology.* 1992;25:102–105.

Soikkeli R, Partanen J, Soininen H, et al. Slowing of EEG in Parkinson's disease. *Electroencephalogr Clin Neurophysiol.* 1991;79:159–165.

Tanaka H, Koenig T, Pascual-Marqui RD, et al. Event-related potential and EEG measures in Parkinson's disease without and with dementia. *Dement Geriatr Cogn Disord.* 2000;11:39–45.

Van Sweden B, Wauquier A, Niedermeyer E. Normal ageing and transient cognitive disorders in the elderly. In: Niedermeyer E, Da Silva FL, eds. *Electroencephalography: basic principles, clinical applications and related fields.* 4th ed. Baltimore: Williams & Wilkins, 1999;340–348.

Yeager CL, Alberts WW, Denature LD. Effect of stereotaxic surgery upon electroencephalographic status of parkinsonian patients. *Neurology.* 1966;16:904–910.

Zijlmans JC, Pasman JW, Horstink MW, et al. EEG findings in patients with vascular parkinsonism. *Acta Neurol Scand.* 1998;98:243–247.

Copyright © 2008 by the American Clinical Neurophysiology Society

ELSEVIER

Neuromuscular Disorders 18 (2008) 215–219

www.elsevier.com/locate/nmd

Expression of caveolar components in primary desminopathy

Akiyo Shinde [a], Satoshi Nakano [a,*], Masashiro Sugawara [b], Itaru Toyoshima [b], Hidefumi Ito [a], Keiko Tanaka [c], Hirofumi Kusaka [a]

[a] *Department of Neurology, Kansai Medical University, 10-15 Fumisono-cho, Moriguchi-city 570-8507, Japan*
[b] *Department of Neurology, Akita University School of Medicine, Akita, Japan*
[c] *Department of Neurology, Brain Research Institute, Niigata University School of Medicine, Niigata, Japan*

Received 11 October 2007; accepted 15 December 2007

Abstract

Myofibrillar myopathies (MFM) involve accumulation of various proteins in the muscle cytoplasm. In myopathy with a heterozygous A337P mutation of the desmin gene, electron-micrographs showed aggregates of vesicular and tubular structures. Positive cytoplasmic reaction for caveolin-3 immunohistochemistry and cholera toxin B binding suggested that caveolae comprised some of the aggregates. As caveolae occur in the Golgi complex and are transported to the cell surface, the results suggest inhibition of their trafficking to the sarcolemma. Alternatively, they could be trapped during internalization. We hypothesize that the accumulation of multiple proteins in MFM could be partially due to inhibited intracellular trafficking.
© 2008 Elsevier B.V. All rights reserved.

Keywords: Myofibrillar myopathy; Desminopathy; Desmin; Caveolae; Distal myopathy; Rimmed vacuole

1. Introduction

Myofibrillar myopathies (MFM) are characterized by focal myofibrillar destruction and pathological accumulations of a variety of proteins, such as muscle intermediate-filament protein desmin in the muscle cytoplasm. Unveiled mutations reside in genes encoding desmin, αB-crystallin, or proteins of Z disks, such as myotilin [1]. Regardless of mutation, MFM show accumulation of myofibrillar and non-myofibrillar proteins. The mechanism of abnormal protein expression remains unclear.

Ultrastructural studies in a patient suffering from MFM with a desmin gene (*DES*) mutation (primary desminopathy) showed aggregates of vesicular structures. To investigate the origin of vesicles, we examined components of T-tubules, sarcoplasmic reticulum and caveolae.

2. Case presentation

The patient's history and postmortem examination focused on the cardiac muscle have been presented elsewhere [2]. Briefly, he had a history of progressive muscle weakness since the age of 45. Around the time of onset, he underwent a muscle biopsy in a hospital and was diagnosed with distal myopathy with rimmed vacuoles. The muscle weakness was initially restricted to the anterior region of the distal legs, but over the years, the weakness spread to his upper extremities and other leg muscles. A cardiac pacemaker was implanted at the age of 51 due to severe conduction defects. From the age of 53, he developed respiratory symptoms. On examination at 54 years old, he had atrophy and weakness that was worse distally than proximally. The results of manual muscle testing in the MRC scale were as follows: deltoid, 3/4 (right/left); triceps brachii, 5/5; finger flexor, 5−/4+; finger extensor, 2/2; quadriceps femoris, 4−/5−; tibialis anterior, 1/1; and gastrocnemius, 2/2. Facial muscles were intact.

* Corresponding author. Tel.: +81 66992 1001; fax: +81 66994 0233.
E-mail address: nakanos@takii.kmu.ac.jp (S. Nakano).

0960-8966/$ - see front matter © 2008 Elsevier B.V. All rights reserved.
doi:10.1016/j.nmd.2007.12.006

3. Mutation analysis

For gene analysis, genomic DNA was extracted upon informed consent from peripheral blood cells according to standard procedures. Sequencing of the UDP-*N*-acetylglucosamine 2-epimerase/*N*-acetylmannosamine kinase gene (*GNE*) [3] and *DES* [4] were analyzed as described previously.

4. Muscle biopsy study

Skeletal muscle biopsy specimens taken from the vastus lateralis muscle at the age of 51 were examined. The specimens were frozen in isopentane cooled in liquid nitrogen. Cryostat sections were prepared and subjected to the routine and immunocytochemical stainings according to a method previously described [5]. Table 1 shows the list of primary antibodies. For electron microscopy, a portion of the muscle specimens was fixed in 5% glutaraldehyde in 0.1% phosphate buffer (pH 7.4), rinsed and postfixed in 2% osmium tetroxide and embedded in resin. Ultrathin sections were stained with uranyl acetate and lead citrate, and examined under a Hitachi H-7000 electron microscope. To detect GM1 ganglioside in lipid rafts, we used a kit and performed the procedure according to the manufacturer's instruction (Molecular Probes, Eugene, OR). Briefly, cryostat sections were incubated in phosphate-buffered saline (PBS) containing 1 μg/mL recombinant cholera toxin B subunit (CTB) conjugated with Alexa Fluor 488 at 4 °C for 10 min, then washed and incubated in rabbit anti-CTB antibody diluted 200-fold with PBS at 4 °C for 15 min to crosslink the CTB-labeled lipid rafts. After washing, the slides were mounted, and viewed with an Olympus photomicroscope (Tokyo, Japan) equipped for epifluorescence.

5. Results

In histochemical analysis of the biopsied muscle, the muscle fiber diameters varied abnormally from 10 to 105 μm. There were marked proliferations of fibrous and fatty connective tissues in the endomysium and perimysium. A proportion of the fibers contained vacuoles. Some vacuoles had purple-red rims on trichrome (rimmed vacuoles). A few fibers contained cytoplasmic bodies or hyaline inclusions on trichrome (Fig. 1A–C). The number of fibers with central nuclei was increased. Scattered fibers showed fiber splitting, as well. Ring fibers were observed. On NADH dehydrogenase-reacted sections, some fibers had a lobulated or a strong subsarcolemmal distribution of enzyme activity. Atrophic fibers showed strong enzymatic activity. Some acid phosphatase activity was present in the cytoplasm or within the vacuoles. On immunohistochemistry, strong immunoreactive products of desmin (Fig. 1D), αB-crystallin, or myotilin were detected in subsarcolemmal regions or deep in the cytoplasm in fibers containing hyaline or other inclusions on trichrome sections. Strong immunopositive deposits of dystrophin were found in the cytoplasm in abnormal fibers (Fig. 1E). Ultrastructural study showed dappled dense structures of Z disk density among the myofibrils, in the subsarcolemmal region, and around vacuoles (Fig. 2A). Dappled dense structures continuous from normal Z disk were sometimes observed. Cytoplasmic collections of vesicles and tubules were occasionally detected (Fig. 2B). Other pathological alterations included vacuoles of various sizes, Z line streaming, mitochondrial aggregation, annular myofibrils, cytoplasmic bodies, spheroid bodies, and myeloid figures. Filaments with a diameter of approximately 15–20 nm were detected in the cytoplasm.

Analysis of nucleotide sequence showed a heterozygous A337P mutation within exon 5 of *DES* (Fig. 1F), which was confirmed by restriction analysis with BsaHI digestion. By screening the 11 coding exons (from exon 2 to exon 12) of *GNE*, nucleotide changes were not identified in the entire coding sequences.

While control specimens showed positive reaction for caveolin-3 and CTB at the sarcolemma, the patient showed caveolin-3 immunoreactive products and CTB-positive deposits in subsarcolemmal regions or deep in the cytoplasm as well (Fig. 1). In dual-color fluorescence study, there was good co-localization between CTB-positive reaction and caveolin-3-positive deposits (Fig. 1J). Deposition

Table 1
List of primary antibodies

Antigen	Type	Clone	Source	Dilution	Purpose
Desmin	MMA	D33	DAKO	1:100	MFM diagnosis
Myotilin	MMA	RSO34	Novocastra	1:20	MFM diagnosis
αB-crystallin	MMA	1B6.1-3G4	Stressgen	1:200	MFM diagnosis
Dystrophin (n-terminus)	MMA	Dy10/12B2	Novocastra	1:5	MFM diagnosis
Vinculin	MMA	VIN-11-5	Sigma	1:50	T-tubule marker
Aquaporin-1	MMA	1/A5F6	UK-serotic	1:50	T-tubule marker
SERCA-1	MMA	VE12,G9	Novocastra	1:50	SR marker
SERCA-2	MMA	IID8	Novocastra	1:50	SR marker
Caveolin-3	MMA	26	BD Transduction	1:100	Caveolae marker

MMA, mouse monoclonal antibody; MFM, myofibrillar myopathy; SR, sarcoplasmic reticulum.

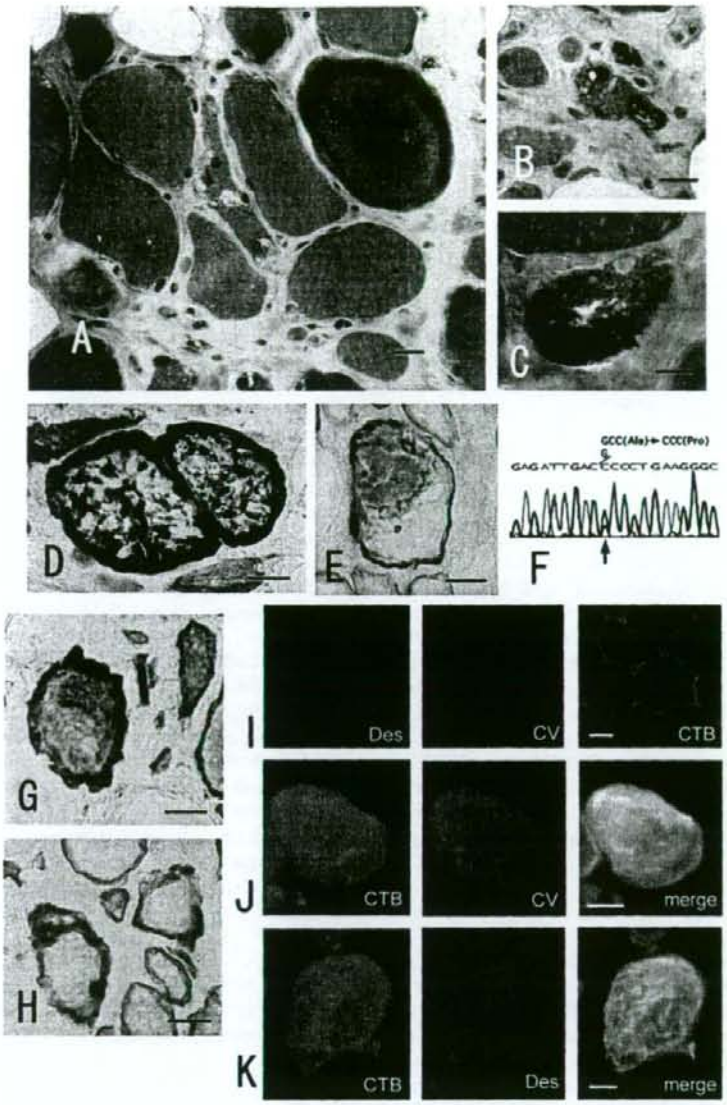

Fig. 1. (A–C) Trichrome-stained frozen sections of the biopsied muscle. (A) A fiber with rimmed vacuoles and those containing focal, diffuse or ring-shaped hyaline inclusions. (B) Typical rimmed vacuoles. (C) Cytoplasmic bodies. (D and E) Immunohistochemistry. Peroxidase method. (D) Desmin and (E) Dystrophin. Desmin-positive materials form thick zones at subsarcolemmal regions and aggregates in the cytoplasm. Dystrophin-positive deposits are present in the cytoplasm as well as sarcolemma. (F) Sequence analysis of the desmin mutation within exon 5, determined by direct sequencing of the PCR products. The position of the point mutation is indicated by the arrow and corresponds to a guanine-to-cytosine transition in the first base of codon 337, resulting in an alanine-to-proline substitution. (G–K) Results of examination of caveolar components. (G and H) Caveolin-3 immunoreactive products were found in subsarcolemmal regions as bands or diffusely in the cytoplasm. (I–K) Dual-color fluorescence study. [Row I] Control. Immunostains for desmin (Des) and caveolin-3 (CV). Localization of cholera toxin subunit B (CTB) reactive products. In each case, positive reaction is seen only at the sarcolemma. (J and K) Patient. [Row J] Localization of CTB-reactive products (green) and caveolin-3 (red) in abnormal fibers. Merging of green and red (merge). Deposits of CTB and caveolin-3 show similar distributions. [Row K] Localization of CTB-reactive products (green) and desmin (red). Merging of green and red (merge). CTB-positive products are found in a desmin-positive fiber. Some co-localization is seen. Bar = 20 μm (A–E, G, H, J and K), 40 μm (I).

of CTB-positive products was usually detected in desmin-positive fibers (Fig. 1K). As for the other antibodies of T-tubules and sarcoplasmic reticulum, we found few or no positive products.

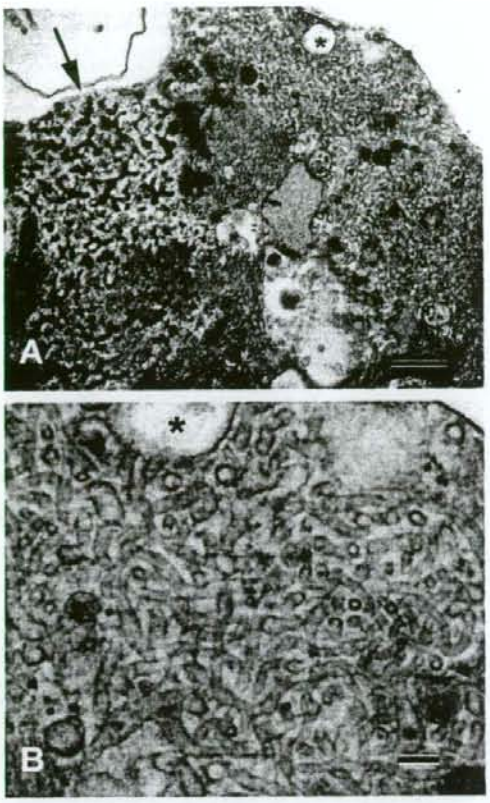

Fig. 2. Electron microscopy. (A) Dappled dense structures (arrow) and collections of vesicular structures beneath vacuolar membranes. (B) A larger magnification of (A). Some vesicles appear to be fused and others show tubular structures. Caveolae can take such configurations [6]. The asterisk indicates the same structure in both pictures. Bar = 0.5 μm (A), 100 nm (B).

6. Discussion

We showed that muscle fibers of primary desminopathy had immunoreactive deposits of caveolin-3 and co-localized CTB-reactive deposits. The results indicate cytoplasmic accumulation of caveolae. Caveolae are small invaginations of the plasma membrane or vesicular organelles. Caveolae can fuse to form grape-like structures and tubules [6]. The collections of vesicular and tubular structures observed under electron microscopy in the present study may be compatible with these profiles of caveolae. Caveolin-3 is the muscle-specific form of caveolins that are the structural proteins of caveolae membrane domains. Caveolae or lipid rafts are enriched in certain lipids, such as GM1 ganglioside of which CTB is a ligand. They represent platforms for membrane protein sorting and construction of signaling complexes. In normal adult skeletal muscle, caveolae are localized at the sarcolemma where caveolin-3 complexes with other sarcolemmal proteins [6]. Whereas we detected the two caveolar markers only at the sarcolemma in normal controls, we detected them also in the cytoplasm in the patient. As caveolae occur at the level of the Golgi apparatus and transfer to the cell surface as vesicles and they are involved in endocytosis or internalization [6], we hypothesize that the cytoplasmic accumulation of caveolae in primary desminopathy is due to inhibition of caveolar trafficking. Primary desminopathy and other MFM show cytoplasmic accumulation of some sarcolemmal proteins, such as dystrophin and sarcoglycans [1]. As is the case with caveolae, they could be stranded and accumulate in the cytoplasm on its way to the sarcolemma after synthesis. As desmin and other types of intermediate-filaments are closely associated with microtubule-based and actin-based motor proteins, which control intracellular trafficking of macromolecules [7], we speculate that disruption of the intermediate-filament network in MFM may inhibit the intracellular trafficking. This may lead to accumulation of a variety of proteins. Detection of proteins of neurodegenerative diseases, such as amyloid precursor protein (APP) and prion protein in MFM [1], might be explained by retention of caveolae, which are rich in APP and involved in processing of prion protein [6].

From the clinical aspect, unlike previously reported patients with the heterozygous *DES* A337P mutation who began with proximal dominant muscle symptoms [8], our patient showed distal dominancy and was initially diagnosed with distal myopathy with rimmed vacuoles (DMRV), which is frequently found in Japan. Moreover, cytoplasmic filamentous inclusions seen on electron microscopy were those in distal myopathy with rimmed vacuoles [9]. Mutation analysis, however, excluded its association. Thus, our case represents a phenotypic difference in the identical *DES* mutation as seen in dysferlinopathy [10]. Although detection of rimmed vacuoles and tubulofilaments is one of the hallmarks of sporadic and hereditary IBMs as well as DMRV, they have been occasionally found in other myopathies, particularly in various distal myopathies [10]. The constellation of morphological findings consisting of rimmed vacuoles, desmin aggregates, tubulofilaments of IBM-type, and dappled dense structures has been described in several papers [11].

Acknowledgement

This work was supported in part by a Grant-in-Aid for Scientific Research from JSPS. We thank Ms. H. Nakabayashi for technical assistance.

References

[1] Selcen D, Engel AG. Myofibrillar myopathies. In: Engel AG, Franzini-Armstrong C, editors. Myology. New York: McGraw-Hill; 2004. p. 1187–202.
[2] Yuri T, Miki K, Tsukamoto R, Shinde A, Kusaka H, Tsubura A. Autopsy case of desminopathy involving skeletal and cardiac muscle. Pathol Int 2007;57:32–6.

[3] Arai A, Tanaka K, Ikeuchi T, et al. A novel mutation in the GNE gene and a linkage disequilibrium in Japanese pedigrees. Ann Neurol 2002;52:516–9.
[4] Sugawara M, Kato K, Komatsu M, et al. A novel de novo mutation in the desmin gene causes desmin myopathy with toxic aggregates. Neurology 2000;55:986–90.
[5] Shinde A, Nakano S, Kusaka H, et al. Nucleolar characteristics of reducing bodies in reducing body myopathy. Acta Neuropathol (Berl) 2004;107:265–71.
[6] Smart EJ, Graf GA, McNiven MA, et al. Caveolins, liquid-ordered domains, and signal transduction. Mol Cell Biol 1999;7:289–304.
[7] Chang L, Goldman RD. Intermediate filaments mediate cytoskeletal crosstalk. Nat Rev Mol Cell Biol 2004:601–13.
[8] Goldfarb LG, Park KY, Cervenakova L, et al. Missense mutations in desmin associated with familial cardiac and skeletal myopathy. Nat Genet 1998;19:402–3.
[9] Nonaka I, Noguchi S, Nishino I. Distal myopathy with rimmed vacuoles and hereditary inclusion body myopathy. Curr Neurol Neurosci Rep 2005;5:61–5.
[10] Udd B, Griggs RC. Distal myopathies. In: Engel AG, Franzini-Armstrong C, editors. Myology. New York: McGraw-Hill; 2004. p. 1169–85.
[11] Fidzianska A, Drac H, Kaminska AM. Familial inclusions body myopathy with desmin storage. Acta Neuropathol (Berl) 1999;97:509–14.

ELSEVIER

Journal of Neuroimmunology 196 (2008) 147–152

Journal of
Neuroimmunology

www.elsevier.com/locate/jneuroim

Soluble tumor necrosis factor receptor 1 and tissue inhibitor of metalloproteinase-1 in hemolytic uremic syndrome with encephalopathy

Masahiro Shiraishi [a], Takashi Ichiyama [a,*], Takeshi Matsushige [b], Takuma Iwaki [c], Kuniaki Iyoda [d], Ken Fukuda [e], Haruyuki Makata [f], Tomoyo Matsubara [a], Susumu Furukawa [a]

[a] *Department of Pediatrics, Yamaguchi University Graduate School of Medicine, Japan*
[b] *Department of Pediatrics, Tokuyama Central Hospital, Japan*
[c] *Department of Pediatrics, Kagawa University Faculty of Medicine, Japan*
[d] *Department of Pediatrics, Hiroshima City Hospital, Japan*
[e] *Department of Pediatrics, Yamaguchi Grand Medical Center, Japan*
[f] *Department of Pediatrics, Yamaguchi Rosai Hospital, Japan*

Received 3 December 2007; received in revised form 22 February 2008; accepted 26 February 2008

Abstract

Enterohemorrhagic *Escherichia coli* (EHEC) induces hemorrhagic colitis and hemolytic uremic syndrome (HUS). Morbidity and mortality are increased in HUS patients with neurologic complications. To determine the pathogenesis of the central nervous system (CNS) involvement in HUS by EHEC, we determined the serum concentrations of interleukin-6 (IL-6), tumor necrosis factor-α (TNF-α), soluble TNF receptor 1 (sTNFR1), IL-10, interferon-γ (IFN-γ), IL-2, IL-4, soluble E-selectin (sE-selectin), matrix metalloproteinase-9 (MMP-9), and tissue inhibitor of metalloproteinase-1 (TIMP-1) during the acute stage in children with HUS with or without CNS involvement. Serum concentrations of IL-6, IL-10, sTNFR1, sE-selectin, MMP-9, and TIMP-1, but not TNF-α, IFN-γ, IL-2, or IL-4, were significantly higher in patients with HUS with encephalopathy compared with controls. Serum IL-6, sTNFR1 and TIMP-1 concentrations were significantly higher in patients with HUS with encephalopathy compared with those with HUS without encephalopathy ($P=0.031$, $P=0.005$, and $P=0.007$, respectively) and those with acute colitis without HUS ($P=0.011$, $P<0.001$, and $P=0.005$, respectively). There were no significant differences in hemoglobin, platelet counts, leukocyte counts, or serum concentrations of IL-10, sE-selectin, MMP-9, aspartate aminotransferase, lactate dehydrogenase, blood urea nitrogen, creatinine, or C-reactive protein between the HUS patients with and without encephalopathy. Our preliminary study suggests that serum IL-6, sTNFR1 and TIMP-1 levels, particularly sTNFR1 and TIMP-1, are important for predicting neurological complications in patients with HUS.
© 2008 Elsevier B.V. All rights reserved.

Keywords: Encephalopathy; Hemolytic uremic syndrome; Soluble tumor necrosis factor receptor; Tissue inhibitor of metalloproteinase-1

1. Introduction

Enterohemorrhagic *Escherichia coli* (EHEC) induces hemorrhagic colitis and hemolytic uremic syndrome (HUS). HUS is a multisystem disease that is characterized by acute renal failure, microangiophathic hemolytic anemia, and thrombocytopenia. The most common cause of HUS is verotoxin-producing *E. coli* represented by the O157 serotype. Neurologic complications involving the central nervous system (CNS) occur in approximately 20% of patients with HUS (Hahn et al., 1989; Siegler, 1994). Common clinical symptoms include seizures and alteration of consciousness, and morbidity and mortality are increased in affected patients (Cimolai et al., 1992; Gallo and Gianantonio, 1995; Hahn et al., 1989; Siegler, 1994). The pathogenesis of the CNS involvement remains unclear.

Cytokines are related to the pathogenesis of various infectious diseases. Interleukin-6 (IL-6) is a cytokine that is well known to play an important role in inflammatory responses. It is recognized as a primary mediator in the pathogenesis of inflammation (Akira et al., 1993; Heinrich et

* Corresponding author. Department of Pediatrics, Yamaguchi University Graduate School of Medicine, 1-1-1 Minamikogushi, Ube, Yamaguchi 755-8505, Japan. Tel.: +81 836 22 2258; fax: +81 836 22 2257.
E-mail address: ichiyama@yamaguchi-u.ac.jp (T. Ichiyama).

0165-5728/$ - see front matter © 2008 Elsevier B.V. All rights reserved.
doi:10.1016/j.jneuroim.2008.02.012

al., 1990). Tumor necrosis factor-α (TNF-α) increases blood-brain vascular permeability, injures vascular endothelial cells, and induces necrosis of myelin and oligodendrocytes (Sato et al., 1986; Salmaj and Raine, 1988). Soluble TNF receptor (sTNFR) is a shedding form of the extra-membranous domain of TNF receptor that can interfere with the function of TNF-α (Seckinger et al., 1990). Interferon-γ (IFN-γ) is produced by T cells and natural killer cells, and influences the class of antibody produced by B cells (Ijzermans and Marquet, 1989). IL-2 is produced by activated lymphocytes and promotes T cell proliferation (Smith, 1984). IL-4 plays an important role in the induction of IgE synthesis, whereas IFN-γ displays an inhibitory effect (Romagnani et al., 1989). IL-10 is an anti-inflammatory cytokine. IL-10 decreases the production of IL-1, IL-6, and TNF-α, induced by an endotoxin or bacterium (Howard et al., 1993; Paris et al., 1997). Adhesion molecules such as E-selectin are primarily found in a soluble form after endothelial cell activation and leukocyte-endothelial cell interaction (Boehme et al., 1996). E-selectin is an endothelial-specific surface protein (Zakeri et al., 2000). Elevated serum levels of soluble E-selectin (sE-selectin) are indicative of vascular endothelial injury (Boehme et al., 1996).

Matrix metalloproteinases (MMPs) constitute a family of enzymes that mediate the degradation of extracellular matrix proteins (Chandler et al., 1997). MMPs play important roles in normal and pathological processes, including embryogenesis, wound healing, inflammation, arthritis, cardiovascular diseases, pulmonary diseases and cancer (Chakraborti et al., 2003). MMP-9 is a member of this family, which is capable of degrading collagen IV, a major component of the basement membrane of the cerebral endothelium, and promotes the migration of cells through tissue or across the blood-brain-barrier (BBB) (Lukes et al., 1999). The activity of MMPs is further controlled by specific tissue inhibitors of metalloproteinases (TIMPs) (Murphy and Knäuper, 1997). TIMP-1 exhibits a high affinity for MMP-9 (Lacraz et al., 1995).

To determine the pathogenesis of the CNS involvement in HUS by EHEC, we determined the serum concentrations of IL-6, TNF-α, sTNFR1, IFN-γ, IL-2, IL-4, IL-10, sE-selectin, MMP-9, and TIMP-1 during the acute stage in children with HUS with or without CNS involvement and acute colitis by EHEC infection.

2. Subjects and methods

Informed consent was obtained from the parents of the patients and control subjects enrolled in this study.

2.1. EHEC infection

Serum samples were obtained from the patients after admission to Yamaguchi University Hospital and five cooperating research hospitals between July 1998 and October 2007. There were 6 patients with HUS with encephalopathy after EHEC infection (5 females/1 male, median age: 5.2 years, range: 17 months–13 years), 10 with HUS without encephalopathy after EHEC infection (6 females/4 males, median age: 6.1 years, range: 18 months–14 years), and 10 with acute colitis by EHEC without HUS (3 females/7 males, median age: 6.3 years, range: 13 months–12 years) (Table 1). The criteria for the diagnosis of EHEC infection included isolation of EHEC from the feces, or a four-fold increase in anti-O157 antibody titer, and/or O157 antigen detection in the feces by latex agglutination test. Twenty-two patients were diagnosed with O157, two with O121, one with O1, and one with O165 infection, respectively.

HUS was defined by the presence of hemolytic anemia, thrombocytopenia, and acute renal failure. HUS with encephalopathy was defined by HUS followed by impaired consciousness with slow activity on electroencephalography with or without seizures. The serum samples were obtained from patients with HUS with encephalopathy on day 2.2±1.0 (range: 1 to 4 days), as the diagnostic day of HUS was considered the first day of illness, 17.8±8.6 h (range: 7 to 30 h) before the onset of neurologic complications, and 5.5±1.2 days (range: 4 to 7 days) after the onset of acute colitis. Serum samples were obtained from the patients with HUS without encephalopathy on day 1.4±0.5 (range: 1 to 2 days), and 5.7±2.2 days (range: 3 to 9 days) after the onset of acute colitis. The serum samples from patients with acute colitis without HUS were obtained 3.7±1.0 days (range: 3 to 5 days) after the

Table 1
Clinical characteristics of the patients with EHEC infection and controls

	HUS with encephalopathy	HUS without encephalopathy	Acute colitis without HUS	Controls for cytokines, sTNFR1, and sE-selectin	Controls for MMP-9 and TIMP-1
Number	6	10	10	73	33
Age					
Median	5.2 years	6.1 years	6.3 years	6.7 years	5.8 years
Range	17 mo–13 years	18 mo–14 years	13 mo–12 years	3 mo–15 years	2–15 years
Sex (F: M)	5:1	6:4	3:7	32:41	18:15
Pathogen	0157 6	0157 7 01 1 0121 1 0165 1	0157 9 0121 1	–	–

EHEC, Enterohemorrhagic *Escherichia coli*; HUS, hemolytic uremic syndrome.

onset of acute colitis. The specimens were frozen at −80 °C until assay.

2.2. Controls

The control subjects for the serum levels of the cytokines, sTNFR1, and sE-selectin were 73 healthy children (32 females and 41 males, aged from 3 months to 15 years; median: 6.7 years) (Ichiyama et al., 2004). The control subjects for the serum levels of MMP-9 and TIMP-1 were 33 healthy children (18 females and 15 males, aged from 2 to 15 years; median: 5.8 years) (Ichiyama et al., 2006).

2.3. Determination of cytokines, sTNFR1, sE-selectin, MMP-9 and TIMP-1 concentrations

The concentrations of IL-6, TNF-α, IFN-γ, IL-2, IL-4 and IL-10 in serum were measured with a cytometric bead array (CBA) kit (BD PharMingen, San Diego, CA) according to the manufacturer's instructions, as described previously (Chen et al., 1999; Ichiyama et al., 2004) with modifications of the data analysis using GraphPad Prism software (GraphPad Prism Software, San Diego, CA). Briefly, the CBA is comprised of a series of beads exhibiting discrete fluorescence intensities at 670 nm. Each series of beads is coated with a monoclonal antibody against a single cytokine, and a mixture of six different series of beads can detect six cytokines in one sample. A secondary phycoerythrin-conjugated monoclonal antibody stains the beads proportionally to the amount of bound cytokine. After fluorescence intensity calibration and electronic color compensation procedures, standard and test samples were analyzed with a FACScan flow cytometer equipped with CellQuest software (BD PharMingen), and the data were transferred to GraphPad Prism. Starting with standard dilutions, the software performed log transformations of the data, and then fitted a curve to 10 discrete points using a four-parameter

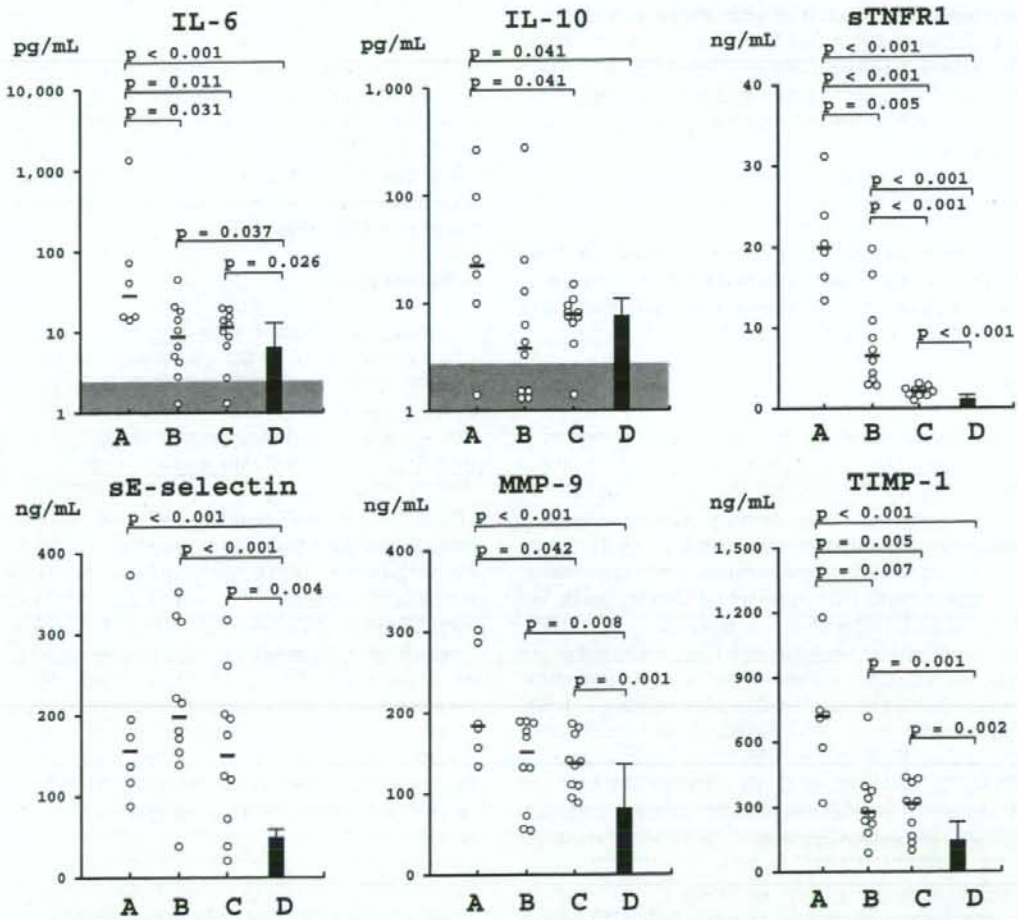

Fig. 1. Serum concentrations of IL-6, IL-10, sTNFR1, sE-selectin, MMP-9, and TIMP-1 in patients with HUS with/without encephalopathy, acute colitis without HUS and controls. A, HUS with encephalopathy (n=6); B, HUS without encephalopathy (n=10); C, acute colitis without HUS (n=10); D, controls. Horizontal lines indicate median values. Shaded areas indicate below the detection limits. Data of controls are presented as the means+1 SD.